Economic Nonlinear Model Predictive Control of Continuous Viral Bioreactors

Available online at www.sciencedirect.com

ScienceDirect

IFAC Papers Online CONFERENCE PAPER ARCHIVE

IFAC PapersOnLine 58-18 (2024) 238–243

Economic Nonlinear Model Predictive Control of Continuous Viral Bioreactors ⋆

Pavan K. Inguva * **Luc T. Paoli** * **Richard D. Braatz** *

* *Massachusetts Institute of Technology, Cambridge, MA 02139, USA (e-mail: inguvakp@mit.edu; lucpaoli@mit.edu; braatz@mit.edu).*

Abstract: Viral particle systems are integral parts of modern biotechnology, finding use in vaccines, drug delivery platforms, and recombinant protein production. Continuous manufacturing of these systems can offer improved manufacturability and quality control. However, viral systems often have complex kinetics which can introduce undesirable process dynamics and lower product titers in continuous operation. This article explores the use of economic nonlinear dynamic optimization and model predictive control to achieve multiple process objectives such as maximizing productivity and/or purity. Economic nonlinear model predictive control is also demonstrated to robustly control the bioreactor under plant-model mismatch in different scenarios.

Keywords: Dynamics and control, Nonlinear process control, Model predictive and optimization-based control, Advanced manufacturing, Industrial biotechnology

1. INTRODUCTION

Viral particle systems include wild-type viruses, viral vectors, and virus-like particles and are integral to modern biotechnology and medicine. These viral systems find use in the production of vaccines (Plotkin, 2014), vaccine adjuvants and antiviral therapeutics (Frensing, 2015), gene therapies (Robbins et al., 1998), and recombinant protein production (Wurm and Bernard, 1999). The limitations of current large-scale viral particle manufacturing processes (e.g., egg-based, fed-batch cell culture processes) (Hegde, 2015) and the advantages of continuous cell-culture processes such as improved productivity, manufacturability, and product quality control have motivated the advancement of continuous manufacturing of viral particles (Gutiérrez-Granados et al., 2018).

The presence of viruses in the bioreactor can introduce complex dynamics to the process arising from viral kinetics, e.g., predator-prey dynamics (Frensing et al., 2013; Inguva et al., 2023; Canova et al., 2023). Figure 1 provides an illustration of the kinetic processes in a simple viral bioreactor. An interesting feature of many viruses, including influenza, is the production of defective interfering particles (DIPs) during replication. These DIPs only contain a portion of the complete viral genome which makes them "defective" in the sense that they can only replicate in cells co-infected with the standard virus (STV) (see Frensing (2015) for an in-depth discussion on DIPs). The presence of DIPs can affect propagation dynamics (Frensing et al., 2013). DIPs are seen as undesirable during production due to their presence adversely impacting productivity (i.e., lower viral titers), introducing undesirable process dynamics, and impacting the biological activity of the final product (Frensing et al., 2013; Frensing, 2015). Continuous bioreactor configurations are also typically more complex than equivalent batch setups which can introduce additional complex process dynamics (Gutiérrez-Granados et al., 2018; Matanguihan and Wu, 2022).

The optimization and control of viral bioreactors can be challenging, and is often done experimentally through classical bioengineering (Gallo–Ramírez et al., 2015; Grein et al., 2017; Fang et al., 2022). For example, strategies to mitigate the impact of DIPs and minimize DIP titers include purifying the virus inoculum, engineering cell lines and virus strains to minimize *de novo* generation of DIPs, and selecting operating conditions that result in low multiplicity of infection (MOI), that is, the ratio of virus particles to host cells (Aggarwal et al., 2011; Frensing et al., 2013; Frensing, 2015).

To date, the use of model-based optimization and control strategies to achieve various process and control objectives for viral bioreactors has not been explored in the literature. Nonlinear model predictive control (MPC), in particular economic nonlinear MPC, can guide the process dynamics along an optimal path, improved disturbance rejection, explicitly account for model uncertainties (Ellis et al., 2014). Nonlinear MPC is well-suited for and has increasingly found successful application in biopharmaceutical manufacturing (Sommeregger et al., 2017; Rathore et al., 2021), and its application to continuous viral particle manufacturing similarly has the potential to improve process operations and facilitate the maturation of continuous manufacturing technologies for viral particles.

In recent work, we explored the dynamics of various bioreactors, including for the production of viral particles, when controlled by simple static output feedback (Proportional control) designed to suppress oscillatory behavior (Inguva et al., 2023). In contrast, here we explore the design and resulting dynamics of much more complex control systems

⋆ Financial support is acknowledged from the Agency for Science, Technology and Research (A*STAR), Singapore.

10.1016/j.ifacol.2024.09.037

– namely, economic nonlinear dynamic optimization and MPC – of a viral bioreactor to achieve a larger set of more complex process aims. Four process and control objectives are considered: maximize bioreactor productivity, enable robust process operation (e.g., model uncertainty), produce a high-purity STV product stream, and identify an optimal startup trajectory. The article is structured as follows. Section 2 outlines the continuous viral manufacturing process and bioreactor model. Section 3 describes the use of open-loop dynamic optimization to optimize the bioreactor. Section 4 demonstrates the use of nonlinear economic MPC to control the bioreactor under plant-model mismatch. The results are summarized in Section 5.

2. VIRAL BIOREACTOR PROCESS AND MODEL

A two-stage continuous stirred-tank bioreactor adapted from Frensing et al. (2013) is considered. The setup consists of a first-stage cell bioreactor used to grow uninfected target cells that are fed into a second-stage virus bioreactor where the viral particles are produced. This configuration decouples the cell growth and viral replication processes. The model equations are adapted from Frensing et al. (2013) and are developed by considering species balances across the viral bioreactor. A schematic of the kinetic processes taking place in a viral bioreactor described by (1) is presented in Fig. 1.

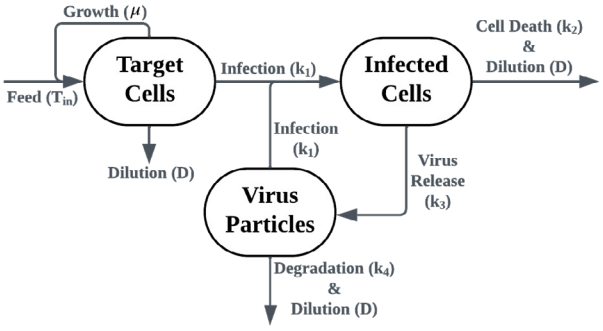

Fig. 1. Schematic of viral kinetics for (1). Similar schematics can be constructed for more complex systems, e.g., see Muller (2015).

Two model variants are considered. The simpler model is

$$\frac{d}{dt}\begin{pmatrix} T \\ I_s \\ V_s \end{pmatrix} = \begin{pmatrix} \mu T - k_1 V_s T + D(T_{in} - T) \\ k_1 V_s T - (k_2 + D) I_s \\ k_3 I_s - k_1 (T + I_s) V_s - (k_4 + D) V_s \end{pmatrix}, \quad (1)$$

where T, I_s, and V_s are the concentrations of the uninfected target cells, cells infected with STVs, and STVs, respectively. A model with more complex dynamics is

$$\frac{d}{dt}\begin{pmatrix} T \\ I_d \\ I_s \\ I_c \\ V_s \\ V_d \end{pmatrix} = \begin{pmatrix} \mu T - k_1 (V_s + V_d) T + D(T_{in} - T) \\ k_1 V_d T - (k_1 V_s - \mu) I_d - D I_d \\ k_1 V_s T - (k_1 V_d + k_2) I_s - D I_s \\ k_1 (V_s I_d + V_d I_s) - k_2 I_c - D I_c \\ k_3 I_s - (k_1 (T + I_d + I_s + I_c) + k_4 + D) V_s \\ k_{33} I_c + f k_3 I_s - (k_1 (T + I_d + I_s + I_c) + k_4 + D) V_d \end{pmatrix}, \quad (2)$$

which incorporates three additional states to account for the presence of DIPs – I_d, I_c, and V_d – which are the concentrations of cells infected with DIPs, co-infected cells, and DIPs, respectively. Both models have two inputs: the bioreactor dilution D and the feed target cell concentration T_{in}. For convenience, the labels "Simplified" and "Full" are used to describe (1) and (2) respectively henceforth. A description of the model parameters and their nominal values for both models can be found in Table 1. The simplified and full models have the initial conditions $(T_0, I_{s,0}, V_{s,0}) = (3{\times}10^6,\ 0,\ 1.25{\times}10^5)$ and $(T_0, I_{d,0}, I_{s,0}, I_{c,0}, V_{s,0}, V_{d,0}) = (3{\times}10^6,\ 0,\ 0,\ 0,\ 0,\ 1.25{\times}10^5)$, respectively. The dilution D and the target cell concentration in the feed T_{in} have nominal values of 0.0396 and $3{\times}10^6$, respectively. A simulation of both models with the nominal initial conditions and parameter values can be found in Canova et al. (2023).

Table 1. Summary of parameters in the viral bioreactor models (1) and (2).

Parameter	Description	Nominal Value	Units
μ	Cell growth rate constant	0.027	$\frac{1}{\text{hr}}$
k_1	STV and DIP infection rate constant	$2.12{\times}10^{-9}$	$\frac{\text{mL}}{\text{virion hr}}$
k_2	Virus-induced cell apoptosis rate constant	$7.13{\times}10^{-3}$	$\frac{1}{\text{hr}}$
k_3	STV production rate constant	168	$\frac{\text{virions}}{\text{cell hr}}$
k_{33}	DIP production rate constant	168	$\frac{\text{virions}}{\text{cell hr}}$
k_4	Virus degradation rate constant	0.035	$\frac{1}{\text{hr}}$
f	Fraction of STV-infected cells that produce DIPs	10^{-3}	–

Local sensitivity analysis on (1) and (2) with the nominal parameter values in Table 1 was performed using the `DiffEqSensitivity.jl` package (Ma et al., 2021) to identify which parameters have the largest effect on the states. To first approximation, for a change in parameter p_i, the impact on state x_j is approximately $\Delta x_j \approx \frac{\partial x_j}{\partial p_i} \Delta p_i$, and the product of the sensitivity and the nominal parameter is taken as the metric for identifying the most sensitive parameters.

For the simplified model (1), the virus infection and STV production rate constants (k_1 and k_3 respectively) have a large impact on the STV concentration V_s during startup, and the STV production and virus degradation constants (k_3 and k_4, respectively) have a large effect on the STV concentration V_s at later times. For the full model (2), the virus infection and STV production rate constants (k_1 and k_3 respectively) similarly have the largest effect on STV concentration V_s during startup, and the DIP production and virus degradation rate constants (k_{33} and k_4, respectively) have the largest impact on the DIP concentration V_d for most times. Given that k_3, k_4 and k_{33}, k_4 have the largest effects for most of the times for the simplified and full models respectively, the impact of uncertainty in those kinetic parameters is explored in Section 4.

3. OPEN-LOOP DYNAMIC OPTIMIZATION

Open-loop dynamic optimization of both the simplified and full models was performed using the `do-mpc` software package (Lucia et al., 2017; Fiedler et al., 2023) which solves the optimal control problem,

$$\begin{aligned} \min_{\mathbf{x},\mathbf{u}} \quad & \int_{t_0}^{t_f} J(\mathbf{x},\mathbf{u})\, dt \\ \text{s.t.} \quad & \dot{\mathbf{x}} = \mathbf{f}(\mathbf{x},\mathbf{u}), \\ & \mathbf{x}(t=0) = \mathbf{x}_0, \\ & \mathbf{g}(\mathbf{x},\mathbf{u}) \leq 0, \end{aligned} \tag{3}$$

where J is the objective function, t_0 and t_f are the initial and final times of the simulation respectively, $\mathbf{x}$ is the vector of states of the system given by (1) and (2) with the corresponding initial condition $\mathbf{x}_0$, $\mathbf{u}$ is the vector of inputs which correspond to the bioreactor dilution D and feed target cell concentration T_{in}, and $\mathbf{g}$ defines the set of constraints on the system. The subscripts ub and lb denote the upper and lower bounds respectively on the state variables and inputs. Non-negativity constraints are imposed on all states and inputs for physical reasons, i.e., $\mathbf{x}_{lb} = \mathbf{u}_{lb} = 0$. The choice of upper bounds is described in the subsequent text. `do-mpc` includes an additional term into the objective function to penalize rapid changes to the inputs: $\mathbf{r}^\top \Delta\mathbf{u}_k^2$, where $\Delta\mathbf{u}_k = \mathbf{u}_k - \mathbf{u}_{k-1}$ and $\mathbf{r}$ is the vector of penalties (Fiedler et al., 2023).

To identify an optimal startup trajectory and maximize the productivity of the bioreactor, an economic objective function was specified. Two scenarios are considered in this work:

(1) Maximize STV production with the simplified model, with D_{ub} set to 0.1 and $T_{in,ub}$ varied. A higher bioreactor dilution corresponds to a larger media consumption, which increases operating costs and, in the case of the simplified model, D_{ub} is sufficient to illustrate the optimal operating strategy. The objective function specified is $J = -DV_s$, as the product of the STV concentration V_s and the dilution D provides a measure for the instantaneous productivity of the system.
(2) Maximize STV production while minimizing DIP production with the full model, with D_{ub} and $T_{in,ub}$ set to 0.25 and 1×10^7, respectively. Two values of the initial condition of the target cell concentration T_0 are considered; the nominal value of 3×10^6 and a reduced value of 1.5×10^6. The objective function specified is $J = -D(V_s - V_d)$, which seeks to maximize dilution D and STV concentration V_s while minimizing DIP concentration V_d.

In both scenarios, the objective function J has units of $\frac{\text{virion}}{\text{hr mL}}$ which corresponds to the viral particle concentration in the product stream normalized by the reactor volume and is a direct measure of the instantaneous productivity. When integrated over the simulation time, the total viral particle yield is obtained. For Scenario 1, the full optimal control problem is solved in a single step, i.e., from $t = t_0$ to $t = t_f$. For Scenario 2, numerical issues related to achieving convergence in the optimization step were encountered when attempting solutions in a single step. Instead, we compute the optimal values of $\mathbf{u}$ sequentially using a receding prediction horizon in a manner equivalent to using MPC in the absence of uncertainty and disturbances.

3.1 Scenario 1

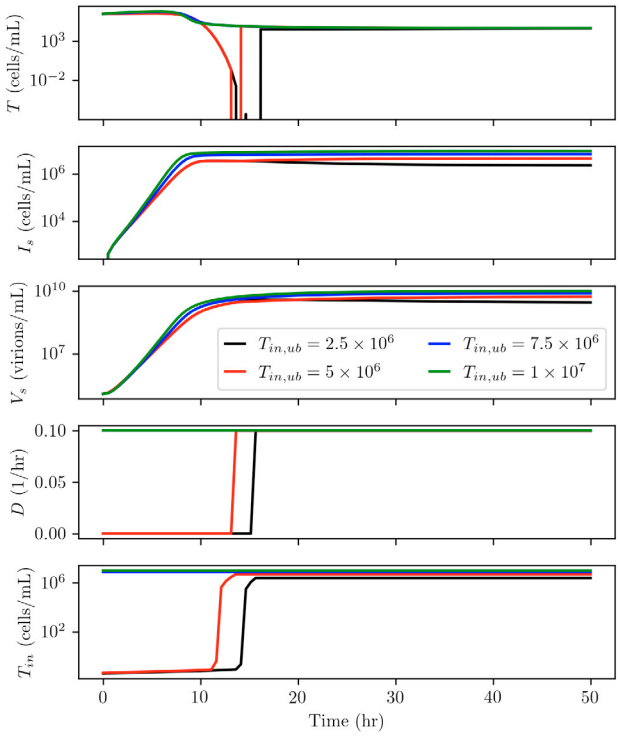

Fig. 2. Numerical solutions to the optimal control problem for Scenario 1 for different values of the maximum allowable feed target cell concentration $T_{in,ub}$.

The optimal control results for varying the maximum allowable feed target cell concentration $T_{in,ub}$ is shown in Fig. 2. For $T_{in,ub} \lesssim T(t=0)$, the optimal startup strategy is to delay feeding any cells and media into the bioreactor (i.e., $T_{in} = D = 0$) to allow accumulation of infected cells and viral particles (I_s and V_s respectively in Fig. 2). For $T_{in,ub} > T(t=0)$, higher productivity is obtained by immediately feeding the bioreactor with media and cells at the maximum possible values, which enables the bioreactor to operate at a higher concentration of target cells as early as possible. In general, the optimal strategy for systems described by the simplified model is to operate at high cell densities and dilution, which may include an initial delay to allow the accumulation of virus particles and infected cells. This control strategy of always operating with both manipulated variables at constraints (i.e., bang-bang control) is easy to implement and understand.

3.2 Scenario 2

This scenario explores the feasibility of employing process controls to obtain a high-purity STV product stream. In the absence of any controls, the model when simulated with nominal parameter and input values predicts that the steady-state concentration of DIPs is much larger than STVs, i.e., $V_d \gg V_s$ (Inguva et al., 2023). As seen in Fig. 3, a suitable trajectory for the feed target cell concentration T_{in} and dilution D can be used to drive the system to

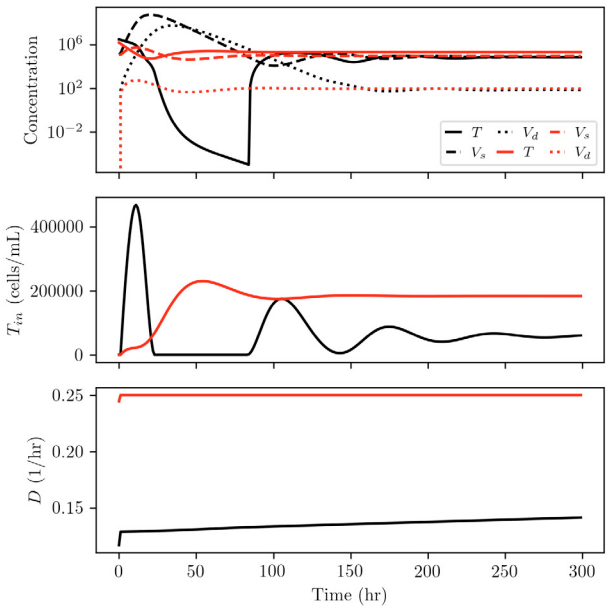

Fig. 3. Dynamic responses obtained from numerical solution of the optimal control problem for Scenario 2 with two values for the initial uninfected target cell concentration T_0 (the red line is for $T_0 = 1.5{\times}10^6$ and the black line is for $3{\times}10^6$).

produce a high-purity STV product stream ($V_s \gg V_d$) while also suppressing oscillatory behaviour. The tradeoff in doing so is that the overall productivity of the system is comparatively low. In effect, this strategy involves operating the bioreactor at a much lower multiplicity of infection (MOI) than the nominal operating conditions, which is a known strategy to minimize DIP production (Aggarwal et al., 2011; Frensing et al., 2013). Similarly, employing at a lower initial uninfected target cell concentration T_0 helps reduce the initial rapid increase in virus particle concentrations (both V_s and V_d) and accelerate the transition of the bioreactor to a state of operation at low MOI.

Considering the comparatively low productivity of such a process, alternative approaches are desired. One such approach is to adopt alternative bioreactor configurations, e.g., tubular flow bioreactors which prevent the accumulation of DIPs along the bioreactor, enabling higher bioreactor productivity while simultaneously generating a high-purity STV product stream (Tapia et al., 2019; Inguva et al., 2023).

4. ECONOMIC NONLINEAR MODEL PREDICTIVE CONTROL

The `do-mpc` package is used to implement economic nonlinear MPC for the two scenarios described in Section 3. We consider plant-model mismatch where the "simulated" plant is different from the model used in the control calculations (given by (1) and (2) with the nominal parameter values).

More specifically, the simulated plant has different values for the most sensitive parameters determined by local sensitivity analysis (see Section 2). Plant-model mismatch of ±50% in the most sensitive parameters is considered. In the `do-mpc` package, the control and prediction horizons are the same and are set to 50 hr for both scenarios while the sampling time is set to 0.5 and 1 hr for Scenarios 1 and 2 respectively.

Considering the sensors available for viral quantification and cell analysis (e.g., see Schwartz and Lowen (2016); Pais et al. (2020); Lomont and Smith (2023)), state-space control for the simplified model (1) is realizable as all three states (i.e., uninfected target cells T, cells infected with STVs V_s, and STVs I_s) are measurable. For the full model (2), a state observer is necessary as distinguishing the different types of infected cells is difficult, making direct measurement of the different infected cell states (i.e., co-infection cells I_c, cells infected with STVs I_s, and cells infected with DIPs I_d) infeasible. In both cases, state-space control establishes a bound on the achievable performance of output feedback-based control.

4.1 Scenario 1

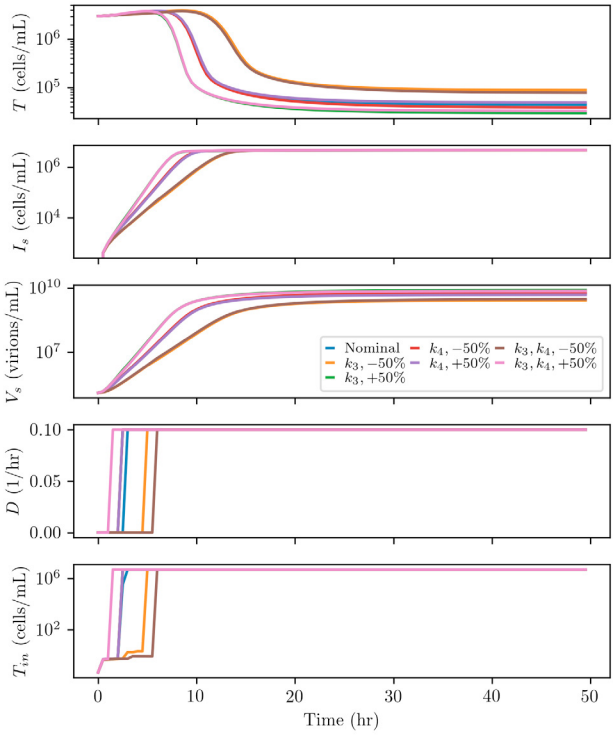

Fig. 4. Dynamic responses for economic nonlinear MPC of the simplified model in Scenario 1 under plant-model mismatch and $T_{in,ub} = 5{\times}10^6$. Uncertainty in the parameters k_3 and k_4 (STV production and virus degradation rate constants, respectively) is considered.

This section considers the effects of uncertainty in the most sensitive parameters k_3 and k_4 (STV production and virus degradation rate constants, respectively) on the economic nonlinear MPC designed for Scenario 1, which aims to maximize the production of STVs for a system described by the simplified model (1). For values of the upper bound on the feed target cell concentration $T_{in,ub}$ larger than about twice the $T(t = 0)$, the closed-loop performance is not significantly affected by the plant-model mismatch, as the optimal operating strategy remains to operate at the highest possible values of the dilution D and feed target

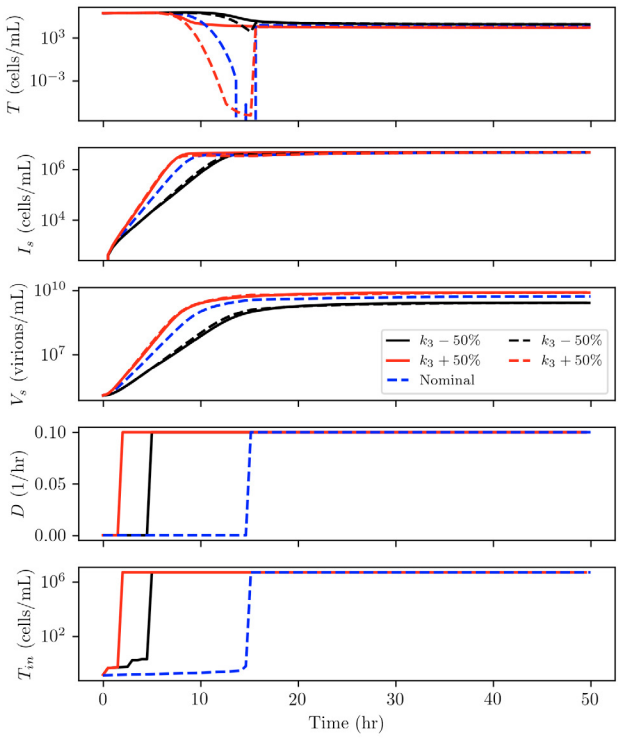

Fig. 5. Comparison of the dynamics responses for open-loop dynamic optimization (dashed lines) and closed-loop economic nonlinear MPC (solid lines) for $T_{in,ub} = 5{\times}10^6$ and $k_3 \pm 50\%$.

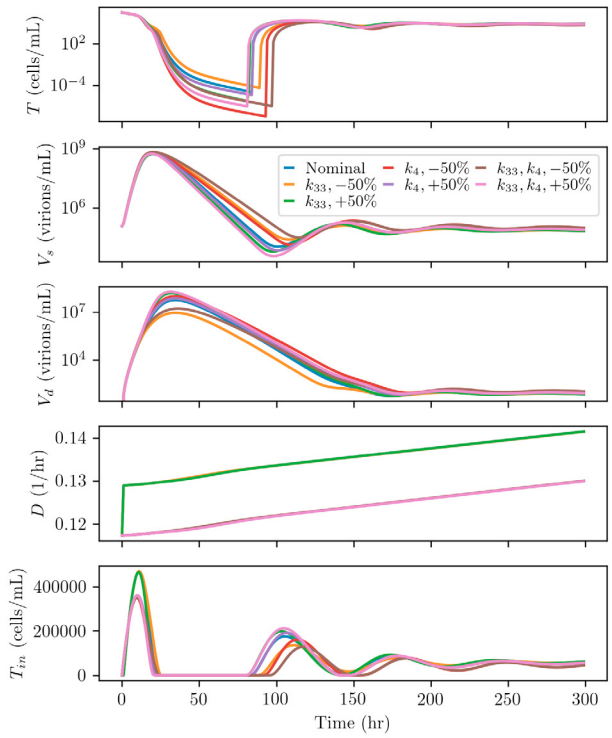

Fig. 6. Economic nonlinear MPC of the full model per Scenario 2 with plant-model mismatch and $T_0 = 3{\times}10^6$. Uncertainty in the parameters k_{33} and k_4 (DIP production and virus degradation rate constants, respectively) is considered.

cell concentration T_{in} from the beginning (plots not shown due to space constraints).

For $T_{in,ub} \lesssim T(t = 0)$, the delay in the feeding of the media and target cells varies slightly, with the controller starting feeding earlier for more productive systems (e.g., $1.5k_3$) and later for less productive systems (e.g., $0.5k_3$), as shown in Fig. 4. In all cases, the onset of controller action (i.e., when the feeding of media and target cells begins) when $T_{in,ub} = 5{\times}10^6$ (as shown in Figs. 4–5) is slightly earlier in closed-loop operation, even under plant-model mismatch, resulting in improved productivity over the open-loop operation (3.6% gain for $0.5k_3$ and 11.7% for $1.5k_3$). This demonstrates that economic nonlinear MPC is indeed a very robust control strategy for Scenario 1.

4.2 Scenario 2

The application of economic nonlinear MPC for the objective function specified in Scenario 2, which aims to maximize the production of STVs while simultaneously minimizing DIPs, is robust in ensuring a high-purity STV product stream under plant-model mismatch in the most sensitive parameters k_{33} and k_4 (DIP production and virus degradation rate constants, respectively) as seen in Fig. 6. In all cases, the oscillatory behaviour is suppressed, which is not surprising considering that the process is driven to operate at a low multiplicity of infection (MOI) as expected from the open-loop dynamic optimization.

5. CONCLUSION

The optimization and control of a two-stage continuous viral bioreactor is explored in this work. When the system does not have DIPs present and can be described by the simplified model, the optimal control strategy to maximize bioreactor productivity, which varies slightly as a function of the upper bound on the feed target cell concentration $T_{in,ub}$, is to operate at maximum T_{in} and dilution D. For lower $T_{in,ub}$, the bioreactor should be operated with zero feed initially, to enable the accumulation of viral particles and infected cells. The simplicity of the control action results in plant-model mismatch having minimal impact on controller performance.

When DIPs need to be considered and the full model provides a more accurate description of the system, the qualitative behavior of the control strategy depends on the performance objective. This work considers the scenario of minimizing DIP production while maximizing STV production to obtain a high-purity STV product stream. The optimal control strategy drives the bioreactor to a state of low multiplicity of infection (MOI), which achieves the desired process objective at the expense of significantly lower productivity. The developed controller is demonstrated to be robust to plant-model mismatch.

REFERENCES

Aggarwal, K., Jing, F., Maranga, L., and Liu, J. (2011). Bioprocess optimization for cell culture based influenza vaccine production. *Vaccine*, 29(17), 3320–3328.

Canova, C.T., Inguva, P.K., and Braatz, R.D. (2023). Mechanistic modeling of viral particle production. *Biotechnology and Bioengineering*, 120(3), 629–641.

Ellis, M., Durand, H., and Christofides, P.D. (2014). A tutorial review of economic model predictive control

methods. *Journal of Process Control*, 24(8), 1156–1178.
Fang, Z., Lyu, J., Li, J., Li, C., Zhang, Y., Guo, Y., Wang, Y., Zhang, Y., and Chen, K. (2022). Application of bioreactor technology for cell culture-based viral vaccine production: Present status and future prospects. *Frontiers in Bioengineering and Biotechnology*, 10, 921755.
Fiedler, F., Karg, B., Lüken, L., Brandner, D., Heinlein, M., Brabender, F., and Lucia, S. (2023). do-mpc: Towards FAIR nonlinear and robust model predictive control. *Control Engineering Practice*, 140, 105676.
Frensing, T. (2015). Defective interfering viruses and their impact on vaccines and viral vectors. *Biotechnology Journal*, 10(5), 681–689.
Frensing, T., Heldt, F.S., Pflugmacher, A., Behrendt, I., Jordan, I., Flockerzi, D., Genzel, Y., and Reichl, U. (2013). Continuous influenza virus production in cell culture shows a periodic accumulation of defective interfering particles. *PLoS ONE*, 8(9), e72288.
Gallo–Ramírez, L.E., Nikolay, A., Genzel, Y., and Reichl, U. (2015). Bioreactor concepts for cell culture-based viral vaccine production. *Expert Review of Vaccines*, 14(9), 1181–1195.
Grein, T.A., Weidner, T., and Czermak, P. (2017). Concepts for the production of viruses and viral vectors in cell cultures. In S.J.T. Gowder (ed.), *New Insights into Cell Culture Technology*. InTech, London, United Kingdom.
Gutiérrez-Granados, S., Gòdia, F., and Cervera, L. (2018). Continuous manufacturing of viral particles. *Current Opinion in Chemical Engineering*, 22, 107–114.
Hegde, N.R. (2015). Cell culture-based influenza vaccines: A necessary and indispensable investment for the future. *Human Vaccines & Immunotherapeutics*, 11(5), 1223–1234.
Inguva, P., Ganko, K., Dubs, A.B., and Braatz, R.D. (2023). Dynamics and control of oscillatory bioreactors.
Lomont, J.P. and Smith, J.P. (2023). In situ process analytical technology for real time viable cell density and cell viability during live-virus vaccine production. *International Journal of Pharmaceutics*, 649, 123630.
Lucia, S., Tătulea-Codrean, A., Schoppmeyer, C., and Engell, S. (2017). Rapid development of modular and sustainable nonlinear model predictive control solutions. *Control Engineering Practice*, 60, 51–62.
Ma, Y., Dixit, V., Innes, M.J., Guo, X., and Rackauckas, C. (2021). A comparison of automatic differentiation and continuous sensitivity analysis for derivatives of differential equation solutions. In *IEEE High Performance Extreme Computing Conference (HPEC)*, 1–9.
Matanguihan, C. and Wu, P. (2022). Upstream continuous processing: recent advances in production of biopharmaceuticals and challenges in manufacturing. *Current Opinion in Biotechnology*, 78, 102828.
Muller, T. (2015). *Population Balance Modeling of Influenza A Virus Replication in MDCK Cells During Vaccine Production*. Ph.D. thesis, Otto-von-Guericke-Universität Magdeburg, Germany.
Pais, D.A.M., Galrão, P.R.S., Kryzhanska, A., Barbau, J., Isidro, I.A., and Alves, P.M. (2020). Holographic imaging of insect cell cultures: Online non-invasive monitoring of adeno-associated virus production and cell concentration. *Processes*, 8(4), 487.
Plotkin, S. (2014). History of vaccination. *Proceedings of the National Academy of Sciences*, 111(34), 12283–12287.
Rathore, A.S., Mishra, S., Nikita, S., and Priyanka, P. (2021). Bioprocess control: Current progress and future perspectives. *Life*, 11(6), 557.
Robbins, P.D., Tahara, H., and Ghivizzani, S.C. (1998). Viral vectors for gene therapy. *Trends in Biotechnology*, 16(1), 35–40.
Schwartz, S.L. and Lowen, A.C. (2016). Droplet digital PCR: A novel method for detection of influenza virus defective interfering particles. *Journal of Virological Methods*, 237, 159–165.
Sommeregger, W., Sissolak, B., Kandra, K., Von Stosch, M., Mayer, M., and Striedner, G. (2017). Quality by control: Towards model predictive control of mammalian cell culture bioprocesses. *Biotechnology Journal*, 12(7), 1600546.
Tapia, F., Wohlfarth, D., Sandig, V., Jordan, I., Genzel, Y., and Reichl, U. (2019). Continuous influenza virus production in a tubular bioreactor system provides stable titers and avoids the "von Magnus effect". *PLoS ONE*, 14(11), e0224317.
Wurm, F. and Bernard, A. (1999). Large-scale transient expression in mammalian cells for recombinant protein production. *Current Opinion in Biotechnology*, 10(2), 156–159.